Validation of High Gradient Magnetic Field Based Drug Delivery to Magnetizable Implants Under Flow

Zachary G. Forbes*, *Member, IEEE*, Benjamin B. Yellen, Derek S. Halverson, Gregory Fridman, Kenneth A. Barbee, and Gary Friedman

***Abstract*—The drug-eluting stent's increasingly frequent occurrence late stage thrombosis have created a need for new strategies for intervention in coronary artery disease. This paper demonstrates further development of our minimally invasive, targeted drug delivery system that uses induced magnetism to administer repeatable and patient specific dosages of therapeutic agents to specific sites in the human body. Our first aim is the use of magnetizable stents for the prevention and treatment of coronary restenosis; however, future applications include the targeting of tumors, vascular defects, and other localized pathologies. Future doses can be administered to the same site by intravenous injection. This implant-based drug delivery system functions by placement of a weakly magnetizable stent or implant at precise locations in the cardiovascular system, followed by the delivery of magnetically susceptible drug carriers. The stents are capable of applying high local magnetic field gradients within the body, while only exposing the body to a modest external field. The local gradients created within the blood vessel create the forces needed to attract and hold drug-containing magnetic nanoparticles at the implant site. Once these particles are captured, they are capable of delivering therapeutic agents such as antineoplastics, radioactivity, or biological cells.**

***Index Terms*—Magnetic drug delivery, magnetic separation cardiovascular disease, stents.**

I. Introduction

CANCER chemotherapeutic agents have been found to have applications in many realms of clinical medicine [1]–[3]. The best approach for localized pathology is to administer drugs only at the site where needed. By delivering the drug locally, the toxicity of the drug to the rest of the body can be reduced while maintaining the desired therapeutic benefit at the site of interest. Thus, the ability to deliver large concentrations of drugs only at the site of interest is of major importance for both the pharmaceutical industry and for clinicians.

Manuscript received March 21, 2006. This work was supported in part by the National Science Foundation under Grant NSF 9984276, the Pennsylvania State Tobacco Fund, and the Philadelphia Nanotechnology Institute. *Asterisk indicates corresponding author.*

*Z. G. Forbes is with the Department of Surgery, Drexel University College of Medicine, 245 N. 15th St., Philadelphia, PA 19102 USA (e-mail: zachary.forbes@drexelmed.edu).

B. B. Yellen was with Drexel University, Philadelphia, PA 19104 USA. He is now with the Department of Mechanical Engineering and Materials Science, Duke University, Durham, NC 27708 USA (e-mail: yellen@duke.edu).

G. Fridman and K. A. Barbee are with the School of Biomedical Engineering, Science, and Health Systems, Drexel University, Philadelphia, PA 19104 USA (e-mail: gg48@drexel.edu; kab33@drexel.edu).

D. S. Halverson and G. Friedman are with the Electrical and Computer Engineering Department, Drexel University, Philadelphia, PA 19104 USA (e-mail: dsh29@drexel.edu; gary@ece.drexel.edu).

Digital Object Identifier 10.1109/TBME.2007.899347

Biological polymers, liposomes, hydrogels, viruses, and other controlled release carriers have been widely investigated [4]–[6]. These vehicles release therapeutic agents under the influence of ultrasound, pH, temperature, or chemical interaction, but in many cases, however, the drug delivery vehicles do not have a mechanism for localization where it is possible to deliver high concentrations of drugs with minimally invasive techniques. This is especially true when repeat dosing is required. The magnetic drug delivery system proposed herein overcomes many of these difficulties, and provides a method for concentrating drugs at selected sites in the body with minimal stress on the patient. This system makes use of the fact that conventional stents, which are implanted in various part of the body, can be modified with a thin layer of magnetic coating or by increasing magnetic precipitates within the stent. Such modifications will render the implant attractive to injected magnetic nanoparticles. A primary example is a cardiovascular stent commonly employed to prevent vessel constriction. In this paper we focus on drug delivery in arterial vasculature, but similar techniques may find applications for other diseases.

A. Stents and Restenosis

Stents are metallic or polymeric tubes made in a wide range of physiologically appropriate diameters and lengths. Currently the most commonly used materials for stents are 316L stainless steel or nickel–titanium (Nitinol) [7]. Stents have been routinely used over the last 15 years in percutaneous transluminal coronary angioplasty (PTCA), a procedure for the treatment of severe, symptomatic coronary stenosis [1]. In-stent restenosis (the re-closing of the vessel) remains a major limitation in coronary stenting. Restenosis is generally considered a local vascular manifestation of the biological response to injury. The injury as a result of catheter insertion and balloon inflation consists of denudation of the endothelium and stretching of the medial smooth muscle [1].

There are several treatment options in practice or under investigation for treating restenosis. Local drug delivery can limit systemic exposure, thereby reducing the risk of systemic toxicity. Techniques for local drug delivery to arterial tissue that have been described include application of drug via local catheter injection, direct coating of the stent with drug, coating of the stent with a drug-containing biodegradable polymer, and hydrogel/drug coating [1]–[3]. Biodegradable stents have also been described [8].

Problems with these technologies, include damage to the polymer layer during implantation (causing portions to sever, break off and cause clot formation), the inability to deliver effective concentrations, one-time dosage limitations, and, in

0018-9294/$25.00 © 2008 IEEE

the case of biodegradable stents, mechanical compromise. An additional concern with the polymer-coated drug-eluting stents is limitation of the endothelialization necessary to cover the stent and prevent the bare metal from coming in long contact with the blood, thereby leading to clot [8].

B. Proposed Design and Comparison to Previous Work

Magnetic targeting of therapeutic agents to specific sites in the body enjoys certain advantages over other drug delivery methods. One advantage is that magnetic colloids can be injected into the bloodstream and guided to the targeted area with external magnetic fields [9]–[13]. This technique, which requires only a simple injection, is far less invasive than surgical methods for targeted drug delivery. Magnetic particles composed of magnetite are well tolerated by the human body [14]. Also, magnetic fields are well suited for biological applications as they are not screened by biological fluids and do not interfere with most biological processes [15]–[18]. Previous attempts to use magnetic particles in these applications have relied on high gradient magnetic fields produced by magnets external to the body to direct magnetic particles to specific locations [9]–[14]. This limits the range of their applications. The main disadvantage of this approach is that externally generated magnetic fields apply relatively small and insufficient local forces on micron and submicron sized particles.

Regardless of the size of the particles or implant, the basic physics of magnetic particle capture is essentially the same. The force on a magnetic particle can be expressed as

$$\vec{F} = \mu_0 V(\vec{M} \cdot \nabla)\vec{H} \tag{1}$$

where $\vec{M}$ is the magnetization of a particle of volume V, subjected to an applied magnetic field gradient, $\nabla\vec{H}$, produced by a magnetic implant. As can be seen from the above equation, two critical factors are responsible for the force on a superparamagnetic particle, namely: 1) the particle's magnetization, which for superparamagnetic materials is proportional to the applied magnetic field; and 2) the magnetic field gradient at the position of the particle [19], [20]

From basic physical principles, it can be shown that a single source cannot simultaneously maximize both the particle magnetizing field and the field gradient in all space. Sources designed to produce strong magnetic field gradients by definition produce field that decays very quickly, and can only magnetize the drug carriers in the immediate vicinity. On the other hand, sources designed to produce far penetrating magnetic fields can effectively magnetize the bulk of the carriers, but can only apply weak forces on the particles because their magnetic field gradient is weak (i.e., its magnetic field decays too slowly). Forces produced by a single magnet decay very quickly because not only does the gradient reduce rapidly with distance away from the magnet, but also the magnetizing field decays quickly.

The novelty of our magnetic targeting system is that it independently controls the magnetizing field and the magnetic field gradient. This drastically reduces the rate at which the magnetic force decays with distance and permits much greater forces to be applied to injected drug carriers. A conceptual drawing of the implant-based magnetic drug delivery system can be found in Fig. 1. The primary focus of our two-source method is an implant-based drug delivery system, which operates by placement of a magnetic implant (a stent or cylindrical endovascular implant) at designated sites in the cardiovascular system and then attracting to the designated sites injected doses of magnetically susceptible drugs. This is accomplished with the aid of a modest and uniform, external magnetic field. This "two source system" allows for independent control over the magnetizing field and the field by using two separate magnetic field sources. One source is designed to produce far-reaching magnetic field in order to increase the magnetization of all the injected carriers to the point of magnetic saturation. Far-penetrating fields are most typically generated with large electromagnets held external to the body. The second magnetic field source is the magnetizable stent providing a high local field gradient when saturated by the external field.

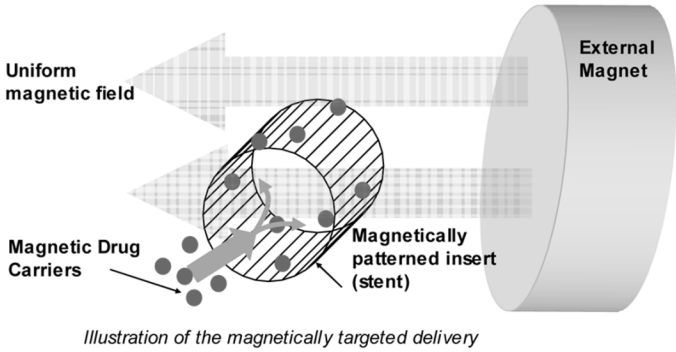


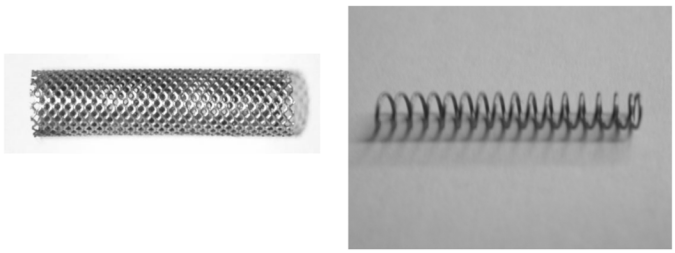
Fig. 1. Conceptual image of a magnetically patterned stent capture injected magnetic particle drug carries under the application of an external magnetic field.

Magnetic microspheres or nanospheres, which can be designed to carry virtually any type of drug or medical agent, are attracted to regions of the strongest magnetic field gradients. Consequently, our research is focused on designing biocompatible implants that produce strong magnetic field gradients near the surface of the implant so that sufficient doses of drug can be captured. One key advantage to this drug delivery system is that the implant can be inserted by minimally invasive techniques such as catheterization, as opposed to surgical techniques used to implant other drug delivery devices. For example, in the treatment of coronary atherosclerosis, the ability to deliver growth-inhibiting drugs to the site of stent implantation can greatly reduce restenosis.

The magnetic force on particles in the cardiovascular system is in competition with drag forces induced by the high flow rate of blood. However, theoretical models predict that the magnetic force applied in our systems can overcome drag forces, leading to significant particle capture. Results from theoretical simulations have provided adequate flow models demonstrating the functionality and effectiveness of magnetic drug delivery systems [21], [22].

C. Ex Vivo Flow Studies

Previous experiments in parallel plate flow chambers demonstrated the ability to capture magnetic particles onto a magnetically plated stainless steel mesh in physiologically significant



(a) (b)

Fig. 2. (a) 304 stainless steel rolled stent. The stent is 5 mm in diameter by 2 cm in length. The wire diameter is 150 μm. (b) 302 stainless steel compression spring. The spring is 3 mm in diameter by 2 cm in length. The wire diameter is 355 μm.

flow rates. A parallel plate flow chamber was designed and machined to accommodate an unrolled stent, consisting of a section of magnetizable stainless steel mesh mounted in a flow system that could mimic the average coronary artery flow velocity of 15 cm/s. Having tested the basic concept, this work will focus on the evaluation of *in vitro*, pipe flow experiments using rolled mesh structures or stainless steel springs. These studies are intended to motivate future *in vivo* experiments and evaluate the potential for delivering controlled dosages of drug onto the implant by examining the ability to capture submicron scale magnetic particles under simulated arterial blood flow conditions.

II. Materials and Methods

A. Stent Material Selection and Electrodeposition

Two different grades of stainless steel were selected as stent-simulating models. The first material selected consisted of molded 304 grade stainless steel (150-μm wire diameter, 450-μm apertures). This material was found to have a larger saturation magnetization than 316L steel, which is commonly used in the manufacture of stents. Stent-like tubes of 304 stainless steel mesh were fabricated by heating the mesh, rolling it into a cylinder (5-mm external diameter and 2-cm length), and joining the overlapping edges using silver solder [Fig. 2(a)]. Although the rolled mesh material comprises a material which is similar in principle to actual stents, the tubes are quite rigid in comparison to commercially manufactured stents.

The second material used to simulate medical device implants was composed of 302 stainless steel compression springs [2-cm-long spring, 3-mm diameter, 355-μm wire diameter; Fig. 2(b)]. These springs are more stent-like in geometry and mechanical properties, but their wire diameter is 3–5 times thicker than struts in a typical stent. These springs are highly magnetic, and probably provide an optimistic estimate for examining different alloys and their inherent abilities to capture particles under the application of external magnetic fields.

Meshes and springs used here as stent models were electroplated with soft magnetic material [23]. Before each electroplating session, a fresh bath was prepared. 100 mL of electroplating solution was prepared consisting of 0.45 M NiCl2, 0.65 M CoCL2, 30 g/dm-3 H3BO3 and a trace of Saccharin (Sigma, MO) [24]. The bath solution was placed in a 1L glass beaker, heated to 55 °C at a pH of 3–3.5, and agitated by an air bubbler fixed at the bottom of the beaker. A Princeton Applied Research 363 Galvanostat/Potentiostat (Princeton Measurements, NJ) was used as the current controller for electroplating. An industrial-grade sheet of cobalt (EMI, CA) 2×2 inches in size was connected as the counter-electrode, and the test material was connected to the working electrode.

TABLE I
Mass-Normalized Saturation Magnetization Data for the Three Selected Model Implant Materials, in Both Plated and Unplated Forms

Saturation Magnetization for Model Implants		
Material	**Plating Height**	**M_s per g**
304 Molded	Unplated	2.97 emu
304 Molded	3.1 μm	11.45 emu
304 Molded	5.2 μm	17.22 emu
302 Spring	Unplated	116.9 emu
302 Spring	2.5 μm	140.4 emu
302 Spring	5.5 μm	155.4 emu

Plating height was determined by measuring the mass of the sample before and after plating, using a digital balance with a resolution of 10-5 grams. Attempts were made to ensure uniform plating by using an air-bubbler kept close to the sample, and periodic rotation of the sample. Based on the sample geometry and density of Cobalt Nickel alloy (assumed to be that of pure Cobalt), the deposited thickness was calculated from the difference in mass after electrodeposition. Two thicknesses of Co/Ni, either 3.1 or 5.2 μm, were deposited onto these rolled mesh materials, with a 0 μm height (unplated) representing the control. Similarly, two separate thicknesses of Co/Ni alloy, either 2.5 or 5.5 μm, were deposited onto the springs, also with a 0 μm height (unplated) representing the control.

B. Magnetic Property Measurements

Mgnetic properties of model implants were measured using a Princeton Measurements MicroMag Alternating Gradient Magnetometer (AGM) (Princeton Measurements, NJ), a highly sensitive instrument for detecting changes in the magnetic properties of materials (Flanders, 1988). The mesh was cut into 5-mm circles using an industrial hole punch. Based on magnetic moment measurements, an effective saturation magnetization of the sample was inferred by normalizing the magnetic saturation to the mass of each sample. Since we were not concerned with inherent material properties, shape effects of the sample wires were not accounted for in saturation magnetization calculations. Five samples of each material were measured by AGM, and the normalized results averaged to obtain Ms per gram (Table I).

C. Magnetic Particle Selection

Commercially available superparamagnetic polystyrene beads (Spherotech, IL) were used in all flow experiments. These beads, composed of 20% γ -Fe2O3 magnetite by weight and labeled with nile red fluorescent pigment, had a nominal diameter of 350 nm with approximately 10% variance in size.

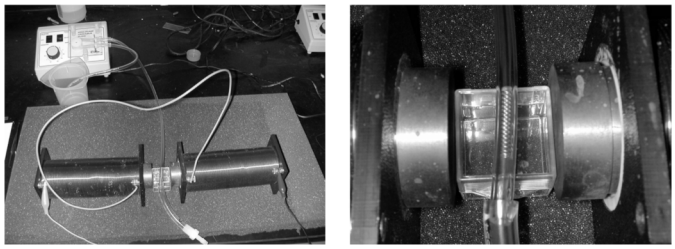


Fig. 3. (left) Broad view of the pipe flow experimental setup, consisting of PVC tubing with an enclosed stent or spring, mounted within a uniform field, and connected to a flow pump. (right) Close up of magnetic mesh in the pipe flow system between two magnetic coils.

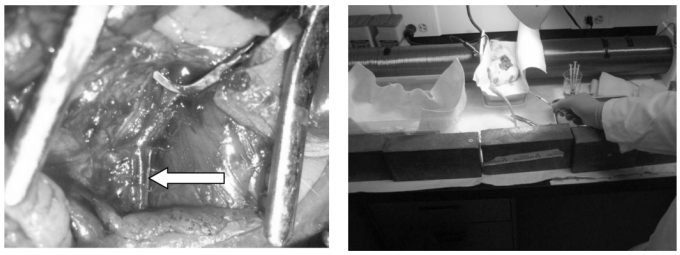


Fig. 4. (left) Surgical image of a placed stent within the common iliac of a Sprague Dawley Rat. (right) After stent implantation and placement of an injection catheter, radiolabeled magnetic particles are injected under exposure to a 0.05T magnetic field.

Particles come in 2 mL water solutions concentrated at 1% w/v or 2.274×109 particles/mL. Specifications from the manufacturer indicate that the magnetic material susceptibility of the particles is on the order of ~ 1–2.

D. Flow Experiments

The pipe flow experimental setup consisted of a 50-mL beaker that supplied the flow pump with solution via a 20-mm-long polyvinyl chloride (PVC) tube (Fig. 3). The pump passes the particle dose through a 60 mm long PVC tube, into which the rolled mesh or spring was gently inserted. The spring is mounted between two solenoid coils with iron cores. Current of 1–5 amperes was passed through the coils with a bipolar operational power supply/amplifier (Kepco, NY) to generate the external magnetic field. In each case, a Lakeshore Model 410 Gaussmeter and Probe (Lakeshore Cryotronics, OH) was used to verify the applied field (most often 500 Gauss). The output of the tubing was captured into a 50-mL centrifuge tube for capture analysis. A variable flow peristaltic pump (Fisher, IL), which produced pulsatile flow, was used for these flow experiments.

For the molded 304 grade steel stent flow experiments, three repetitions were performed for each plating thickness: 0 (unplated), 3.1, and 5.2 μm of Co/Ni. It should be noted that unplated 304 steel still maintains inherent paramagnetic properties, increased by plated layers. For all flow experiments using the 5-mm molded stents, a PVC tube with 5mm inner diameter was selected to be consistent with the outer dimensions of the rolled stent. A 25-mL solution of magnetic particles in deionized water at 1% by volume particle concentration was selected as the first dose size. The sample was vortexed for 10 s immediately before delivery to ensure uniform suspension. Before experiments began, the magnetic field was turned on, and a 25-mL priming dose of DI water was passed through the system. The particle concentration was then introduced, followed by a 25-mL rinse with DI water in the continued presence of the applied magnetic field. The 50-mL sample of flow experiment output and rinse water was kept in a 50-mL centrifuge tube and stored at 4 °C for analysis.

For the compression spring flow experiments, again three repetitions were performed for each plating thickness: 0 (unplated), 2.5, and 5.5 μm of Co/Ni. For all flow experiments using the 3-mm springs, an approximately 3 mm in diameter polyethylene tube was selected to fit the outer dimensions of the spring. A 10-mL solution of magnetic particles in deionized water at 1.0% by volume particle concentration was vortexed for 10 s immediately before delivery. Before experiments began, the magnetic field was turned on, and a 10-mL priming dose of DI water was passed through the system. The particle concentration was then introduced, followed by a 10-mL rinse with DI water in the continued presence of the applied magnetic field. The 20-mL sample of flow experiment output and rinse water was kept in a 50-mL centrifuge tube and stored at 4 °C for analysis.

E. AGM Analysis of Capture Efficiency

Flow output for each experiment was collected in a centrifuge tube and refrigerated. Before each experiment had been performed, a control sample of the input dose was prepared to compare to flow output results. Each tube of flow output was vortexed for 10 s to resuspend the particles, and a 5-μL sample was added to a 5-mm-diameter glass cover slip. The slips were allowed to dry for one hour and then analyzed in the AGM [25]. Five samples of each flow experiment were measured and then compared to the magnetic measurement for the input sample for each experimental concentration. The AGM has a $\pm 2.0\%$ error.

F. Preliminary in Vivo Work

Under approved IACUC protocol 03446, rat angioplasty was performed on 400g large adult Sprague Dawley rats. 302 grade stainless steel compressions springs (1-mm diameter by 5-mm length) were inserted into the iliac artery. Spherotech magnetic particles, as described above, were labeled with Technetium-99m for quantification of capture as well as gamma imaging. Rats were exposed to a 0.05T uniform magnetic field for 5 min while injected with the radiolabeled dose of magnetic particles concentrated in 1 mL of normal saline. Instant thin layer chromatography was used to evaluate the efficiency of the radiolabeling technique, in addition to the preparation of an equal standard dose for every study. This allows individual experiment determination of radioactivity per particle injected for accurate quantification of capture and biodistribution data. In Fig. 4, surgical placement of the stent, as well as the magnetic injection setup, are seen.

III. Results

A. Molded Stent Flow Results

A fluorescent image of a 304 stent with captured 350-nm-diameter superparamagnetic particles can be seen in Fig. 5. These

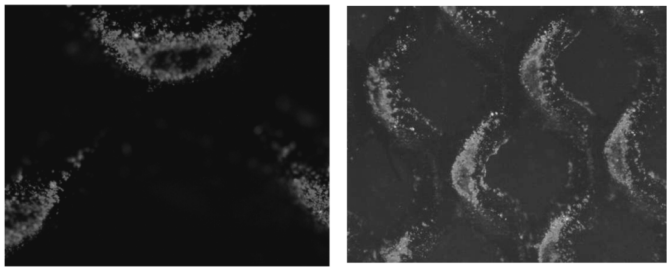


Fig. 5. 5x (left) and 10x (right) images of densely captured 350nm particles on a 304 Stainless Steel mesh. (left) Flow is in the upward direction of the image. (right) Flow is applied towards the right of the image.

TABLE II
CAPTURE RESULTS FOR 5-mm DIAMETER 304 GRADE STEEL MOLDED STENT FLOW EXPERIMENTS WITH 25-mL DOSES AT 1.0% BY VOLUME CONCENTRATION OF 350 nm MAGNETIC PARTICLES. RESULTS ARE GIVEN IN PERCENTAGE OF CAPTURE OF THE TOTAL PARTICLE DOSE, AND THE APPROXIMATE NUMBER OF CAPTURED PARTICLES. ALTERNATING GRADIENT MAGNETOMETER ERROR IS $\pm 2.0\%$

Capture Results for 304 Stainless Steel Molded Stents		
Plating Height	**% Capture**	**Numerical Capture (x 10^9)**
Unplated	6.8 %	8.16
3.1 μm	14.3 %	17.2
5.2 μm	15.9 %	19.08

flow experiments were only performed for a particle concentration of 1.0% by volume, but demonstrated that for a large diameter implant, at physiologically significant flow velocity for the vessel diameter (based on average coronary output), magnetic nanoparticles can be captured. Table II provides the percentage of capture for unplated, as well as CoNi plating heights of 3.1 and 5.2 μm. Results are given in percentage of capture of the total particle dose, and the approximate number of captured particles.

B. Compression Spring Flow Experiments

These flow experiments were performed for particle concentrations of 1.0% by volume. For an average coronary artery scaled implant at physiologically relevant flow velocity, magnetic nanoparticles can be captured. Table III provides the percentage of capture for unplated, as well as CoNi plating heights of 2.5 and 5.5 μm. Results are given in percentage of capture of the total particle dose, and the approximate number of captured particles.

Fig. 6 shows characteristic fluorescent images for each plating height for experiments performed at a 1.0% by volume concentration of 350-nm magnetic particles. Images can be seen of the outside and inside of the spring. Due to the density of capture, by inspection, it is difficult to differentiate between the three samples.

C. Selected in Vivo Results

Rat studies have been completed at increasingly scaled down dose sizes due to the success of targeting. The most desirable end is minimizing the amount of magnetic material necessary to obtain maximum therapeutic results.

TABLE III
THIS TABLE PRESENTS EXPERIMENTAL RESULTS FOR 302 STAINLESS STEEL COMPRESSION SPRINGS THAT ARE UNPLATED, AND AT CO-NI PLATING HEIGHTS OF 2.5 AND 5.5μm, FOR A DOSE CONCENTRATION OF 1.0% 350 nm MAGNETIC PARTICLES BY VOLUME IN DEIONIZED WATER. RESULTS ARE GIVEN IN PERCENTAGE OF CAPTURE OF THE TOTAL PARTICLE DOSE, AND THE APPROXIMATE NUMBER OF CAPTURED PARTICLES. ALTERNATING GRADIENT MAGNETOMETER ERROR IS $\pm 2.0\%$

Spring Flow Results – 1.0 % Particle Concentration		
Plating Height	**% Capture**	**Numerical Capture (x 10^9)**
Unplated	12.6 %	6.05
2.5 μm	15.6 %	7.49
5.5 μm	16.3 %	7.82

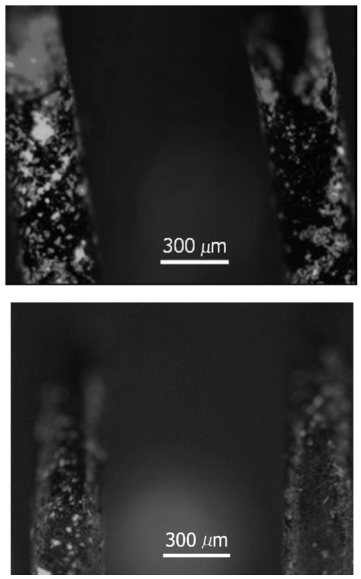


Fig. 6. 5x objective fluorescent images of captured 350 nm rhodamin-stained magnetic particles on 302 stainless steel springs from pipe flow experiments. (top) Image: unplated spring. (bottom) Image: 5.5 μm CoNi plated spring.

Fig. 7 shows a gamma camera image of a 395g rat which received a 4 mg/kg dose of magnetic particles under 5 min of exposure to a 0.05 Tesla uniform magnetic field. The red arrow points to the implanted stent location, demonstrating a "hot spot" from its captured magnetic material content. Particles were labeled at greater than 90% efficiency with Technetium-99m, verified by thin layer chromatography. Fig. 8 shows the biodistribution of magnetic particles within various tissues of the rat. Organ harvesting and weight normalization was combined with measurement of a dose standard to determine the amount of radioactivity per delivered magnetic particle.

IV. DISCUSSION

As predicted from previous studies [12], a stent model of 304 grade stainless steel is capable of magnetically capturing signif-

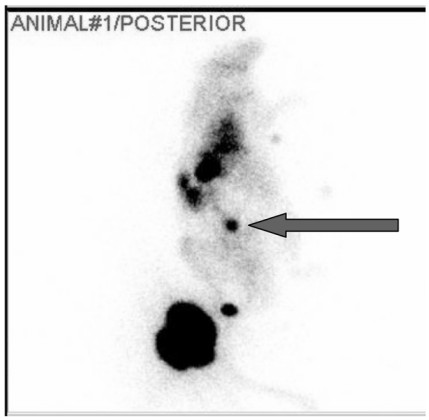


Fig. 7. Gamma image of captured particles to an implanted magnetic spring, noted by the arrow. The large mass to the lower left is the liver, removed and placed aside for clarity.

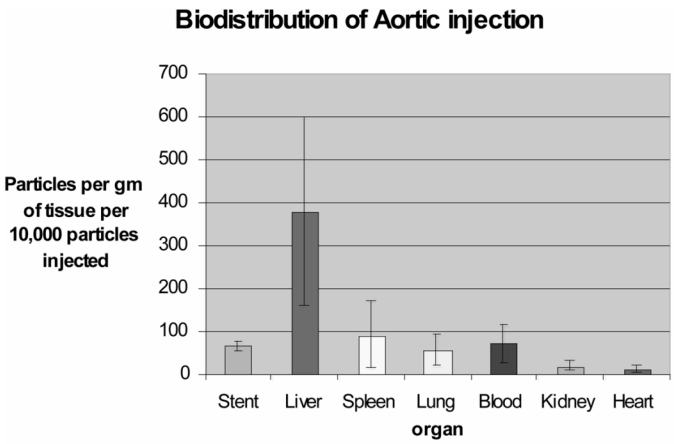


Fig. 8. Biodistribution of uncaptured particles per gram of tissue. Early studies found the liver to peak in the short term, but to drop to lower levels after long exposure to the applied magnetic field, indicating a long circulation life for the used magnetic particles.

icant numbers of 350 nm magnetic particles without the addition of a plated layer of soft magnetic alloy. Upon addition of a 3.1 μm plating layer, the saturation magnetization of the device is increased to four times that of an unplated sample, but roughly only a doubling of capture occurs. Further plating to a 5.2 μm height shows just a little over 10% increase in capture. These results indicate that the capturing abilities of the applied magnetic forces are beginning to level off at the 17 emu/g normalized saturation magnetization for this particular material and geometry. Our prior theoretical models predicted that particles flowing in the center of the vessel are much more difficult to capture, and the plateau phenomena seen in numerical capture most likely relates to an inability to magnetically force these particles' trajectories rapidly enough to trap them on the surface of the stent, even with significant magnetic features upon it.

It is not surprising that an unplated 302 grade stainless steel compression spring, with its high saturation magnetization, is able to capture significant amounts of magnetic nanoparticles. Due to the inherently high saturation magnetization of these springs, very little benefit in terms of capture was obtained by the addition of the two different plating heights of soft magnetic alloy. Even when considering potential error due to loss of particles to the tubing, or the limitations of the AGM measurement procedure, the dose concentration of 1.0% provided extremely dense capture. Based on the free length and wire diameter of these springs, they contain a total surface area of 1.93 cm^2. Idealizing and neglecting the points of contact with the vessel wall and if each particle is modeled as a cube with a 350-nm side, 1.57×109 particles would be necessary to provide a uniform, single particle layer coating. Capture by the unplated spring at concentration was nearly four times that amount.

In our first *in vivo* studies, for a 300-nm or greater particle, it is not surprising to find a large distribution within the liver. We were pleased to find that the lung distribution was low, and that the blood distribution remained high. This demonstrates that the particles have a long circulation life. While the studies to this point only focus on local injection, the circulation data points increasingly to the legitimacy of intravenous injection as a means for particle delivery to the implant. It should also be noted that high activity in the liver is also reflective of the large blood content within the organ, and early results at particle sizes of 100nm are showing particle excretion from the liver into the duodenum. Future studies will optimize This will aid in demonstrating that the particles do not pose a risk of thombosis in the liver or other tissues.

V. Conclusion

In summary, for a range of stent-like structures 3 to 5 mm in diameter, with different geometries, and for normalized saturation magnetizations from 3 to 150 emu/g, magnetic particles were successfully captured at significant numbers. While a material with such a high saturation magnetization as 302 grade stainless steel may never be used for an endovascular implant, it provided an opportunity to test the upper bounds of the full latitude of the capture method, *in vitro* and *in vivo*. Strongly paramagnetic or ferromagnetic stents would be impractical due to the inability to safely perform MRI procedures on the patient in the future. Such materials would be at risk of torquing within these large fields. As this technology claims preventive and long term advantages, it is crucial to find a functional middle ground between magnetic targeting capabilities and the safe use of MRI technology for other pathology. As a result, we continue to evaluate the deposition of soft magnetic alloy micro-features onto otherwise nonmagnetic 316L (the current standard metal for coronary stents) in order to meet both of these needs. Additionally, we are working with magnetic coatings that also allow for proper expansion and mechanical behavior required for the stent's primary functionality. These may be chemically passivated to further limit metallic ion leaching already commonly seen with the use of bare metal stents. The results presented here further validate the hypothesis that the method could be successful by adjusting the amount of magnetic precipitates dispersed within a stent itself, or by the addition of small, soft magnetic features.

While we continue to evaluate dose ranges, magnetic field exposure time, and administration route in rats, we have begun the design of 316L grade stainless steel stents with electroplated magnetic features for larger animal models. We propose the extension of our flow experiments to *in vivo* testing in New Zealand White Rabbit (Drexel IACUC #16182 Study of Magnetic Nano-sphere Delivery to a Magnetizable Stent).,

in which human scale magnetic stents can be implanted in order to complete the milestones proposed. These stents have been designed at Drexel University and are in early stages of preparation by a suitable third party. In vivo results balanced with clinical perspective and engineering design will provide the appropriate input to selection of the optimal grade of steel or magnetic coating material and particle composition. It is the intent to rationally develop an understanding of all parameters and risk so that the technology can be easily adapted to existing implant designs for any of the above mentioned applications, with cardiac stents as the desired entry point.

ACKNOWLEDGMENT

The authors would like to acknowledge Drexel Biomedical Engineering graduate student D. Hansberry for preparation of magnetic coils and Drexel Surgery Residents F. Stoddard, M.D., W. Anjum, M.D., S. Jagtap, M.D., and M. Pekarev, M.D., for their assistance during *in vivo* trials.

REFERENCES

[1] S. M. Garas, "Overview of therapies for prevention of restenosis after coronary interventions," *Pharmacol. Therapeutics*, vol. 92, pp. 165–78, 2001.

[2] J. Garibaldi and B. J. Hogg, "Magnetic vascular defect treatment system," U.S. Patent 6 315 709, Nov. 13, 2001.

[3] A. H. Gershlick *et al.*, "Treating atherosclerosis: local drug delivery from laboratory studies to clinical trials," *Atherosclerosis*, vol. 160, pp. 259–271, 2002.

[4] P. A. Dijkmans, "Microbubbles and ultrasound: from diagnosis to therapy," *Eur. J. Echocardiogr.*, vol. 5, no. 4, pp. 245–256, 2004.

[5] R. D. Hofheinz *et al.*, "Liposomal encapsulated anti-cancer drugs," *Anti-Cancer Drugs.*, vol. 16, no. 7, pp. 691–707, 2005.

[6] M. S. Lesniak *et al.*, "Novel advances in drug delivery to brain cancer," *Technol. Cancer. Res. Treat.*, vol. 4, no. 4, pp. 417–428, 2005.

[7] E. Regar *et al.*, "Stent development and local drug delivery," *Br. Med. Bull.*, vol. 59, pp. 227–248, 2001.

[8] R. S. Schwartz *et al.*, "Drug-eluting stents in preclinical studies. Recommended evaluation from a consensus group," *Circulation*, vol. 106, pp. 1867–1873, 2002.

[9] G. A. Flores, "In-vitro blockage of a simulated vascular system using magnetorheological fluids as a cancer therapy," *Eur. Cells Mater.*, vol. 3, pp. 9–11, 2002.

[10] J. M. Gallo *et al.*, "Preclinical and clinical experiences with magnetic drug targeting," *Cancer Res.*, vol. 57, pp. 3063–3064, 1997, Correspondence re:.

[11] A. S. Lübbe, C. Alexiou, and C. Bergemann, "Clinical applications of magnetic drug targeting," *J. Surg. Res.*, vol. 95, pp. 200–206, 2001.

[12] K. Mossbach and U. Schroder, "Preparation and characterization of magnetic polymers for targeting of drugs," *FEBS Lett.*, vol. 102, pp. 112–116, 1979.

[13] S. Rudge *et al.*, "Adsorption and desorption of chemotherapeutic drugs from a magnetically targeted carrier (MTC)," *J. Controlled Release*, vol. 74, pp. 335–340, 2001.

[14] M. Babincova, P. Babinec, and C. Bergemann, "High-gradient magnetic capture of ferrofluids: Implications for drug targeting and tumor embolization," *Zeitschrift für Naturforschung*, vol. C, pp. 909–911, 2001.

[15] G. B. Bell, A. A. Marino, A. L. Chesson, and F. A. Struve, "Human sensitivity to weak magnetic fields," *The Lancet*, vol. 338, pp. 1521–1522, 1991.

[16] J. L. Kirschvink, A. Kobayashi Kirschvink, J. C. Diaz-Ricci, and S. J. Kirschvink, "Magnetite in human tissues: A mechanism for the biological effects of weak ELF magnetic fields," *Bioelectromagnetics*, pp. 101–113, 1992, Suppl. 1.

[17] L. Sakhnini and R. Khuzaie, "Magnetic behavior of human erythrocytes at different hemoglobin states," *Eur. Biophys. J.*, vol. 30, pp. 467–470, 2001.

[18] J. F. Schenck, "Safety of strong, static magnetic fields," *J. Mag Res. Imaging*, vol. 12, pp. 2–19, 2000.

[19] F. J. Friedlaender, "Particle motion near and capture on single spheres in HGMS," *IEEE Trans. Magn.*, vol. MAG-17, no. 6, pp. 2801–2803, Nov. 1981.

[20] F. J. Friedlaender, "Particle buildup on single spheres in HGMS," *IEEE Trans. Magn.*, vol. MAG-17, no. 6, pp. 2804–2806, Nov. 1981.

[21] Z. G. Forbes, B. B. Yellen, K. A. Barbee, and G. Friedman, "An approach to targeted drug delivery based on uniform magnetic fields," *IEEE Trans. Magn.*, vol. 39, no. 5, pp. 3372–3377, Sep. 2003.

[22] B. B. Yellen, Z. G. Forbes, D. S. Halverson, G. Fridman, K. A. Barbee, M. Chorny, R. Levy, and G. Friedman, "Targeted drug delivery to magnetic implants for therapeutic applications," *J. Magn. Magn. Mater.*, vol. 293, no. 1, pp. 647–654, 2005.

[23] F. A. Loweinheim, *Electroplating*. New York: McGraw-Hill, 1978.

[24] M. Duch, "Electrodeposited Co-Ni alloys for MEMS," *J. Micromech. Microeng.*, vol. 12, pp. 400–405, 2002.

[25] P. J. Flanders, "An alternating-gradient magnetometer," *J. Appl. Phys.*, vol. 63, no. 8, pp. 3940–3945, 1988.

Zachary G. Forbes (M'06) was born in New Glasgow, Nova Scotia, Canada, on August 8, 1979, and naturalized as a United States citizen in 1995. He received the B.S.E. degree in biomedical engineering with a focus on vaginal drug delivery from Duke University, Durham, NC, in 2000, the M.S. degree in biomedical engineering from Drexel University, Philadelphia, PA, in 2003, and the Ph.D. degree in biomedical engineering in 2005 also from Drexel University with a focus on magnetic drug delivery stents.

His research focus is on therapeutic applications of magnetic nanoparticles and magnetizable implants for various pathology including the treatment of arterial restenosis and magnetic targeting of antibiotics to infected orthopedic implants.

Dr. Forbes is a member of the IEEE EMBS, the Biomedical Engineering Society, the International Society for Cell Therapy, and an Affiliate of the American College of Surgeons.

Benjamin B. Yellen, photograph and biography not available at the time of publication.

Derek S. Halverson, photograph and biography not available at the time of publication.

Gregory Fridman, photograph and biography not available at the time of publication.

Kenneth A. Barbee, photograph and biography not available at the time of publication.

Gary Friedman, photograph and biography not available at the time of publication.